Wuhan University
Journal of Natural Sciences

2022, Vol.27 No.4, 313-320

Article ID 1007-1202(2022)04-0313-08
DOI https://doi.org/10.1051/wujns/2022274313

The Space-Time Meshless Methods for the Solution of One-Dimensional Klein-Gordon Equations

ZHANG Zhiqiang[1], WANG Fuzhang[2]†, ZHANG Juan[3,4]

1. General Education Center, Zhengzhou Business University, Gongyi 451200, Henan, China;
2. School of Mathematics and Statistics, Xuzhou University of Technology, Xuzhou 221018, Jiangsu, China;
3. School of Computer Science & Technology, Huaibei Normal University, Huaibei 235000, Anhui, China;
4. School of Information and Control Engineering, China University of Mining and Technology, Xuzhou 221116, Jiangsu, China

Abstract: A simple direct space-time meshless scheme, based on the radial or non-radial basis function, is proposed for the one-dimensional Klein-Gordon equations. Since these equations are time-dependent, it is worthwhile to present two schemes for the basis functions from radial and non-radial aspects. The first scheme is fulfilled by considering time variable as normal space variable, to construct an "isotropic" space-time radial basis function. The other scheme considered a realistic relationship between space variable and time variable which is not radial. The time-dependent variable is treated regularly during the whole solution process and the Klein-Gordon equations can be solved in a direct way. Numerical results show that the proposed meshless schemes are simple, accurate, stable, easy-to-program and efficient for the Klein-Gordon equations.

Key words: radial basis functions; meshless method; space-time
CLC number: O 242

Received date: 2022-03-21
Foundation item: Supported by Anhui Provincial Natural Science Foundation (1908085QA09)
Biography: ZHANG Zhiqiang, male, Associate professor, research direction: computational physics. E-mail: zhangzhiqiang08@gmail.com
† To whom correspondence should be addressed. E-mail: wangfuzhang1984@163.com

0 Introduction

The mathematical formulation and subsequent assistance in the resolution of physical and other problems involving functions of multiple variables, such as the propagation of heat or sound, fluid flow, elasticity, electrostatics, and electrodynamics, are made possible by the use of partial differential equations[1-3]. After the first report by Cajori Florian in the year 1928 on partial differential equations (PDEs), partial differentiation and integration, there have been different kinds of PDEs. A large number of mathematical models in mathematical physics can be described by the one-dimensional Klein-Gordon equations. It has attracted much attention in studying classical and quantum mechanics, solitons and condensed matter physics[4,5].

For such problems, it is almost impossible to get the analytical solutions[6-9]. Thus one should consider numerical approximations to the Klein-Gordon equations. A variety of numerical techniques have been developed and compared for solving the Klein-Gordon equations[10-14]. These numerical techniques are based on the finite difference schemes[15] or spectral and pseudo-spectral methods[16,17].

To avoid the mesh generation, the traditional radial-basis-function-based meshless methods have attracted the attention of researchers[18-20]. Based on the Thin Plate Splines radial basis functions and the cubic B-spline scaling functions, Dehghan and his coworkers[21,22] proposed numerical schemes to solve the one-dimensional nonlinear Klein-Gordon equation with quadratic and cubic nonlinearity. Dehghan and Mohammadi[23] proposed two numerical meshless techniques based on radial basis functions and the method of generalized moving least squares for simulation of coupled Klein-Gordon-Schrodinger equations. The spectral meshless radial point interpolation technique is applied to obtain the solution of two- and three-dimensional coupled Klein-Gordon-Schrodinger equations by Shivanian and Jafarabadi [24]. Very recently, Ahmad *et al*[25] proposed a local meshless differential quadrature collocation method based on radial basis functions for the numerical simulation of one-dimensional Klein-Gordon equations. These traditional numerical techniques are based on two-level finite difference approximations. A direct meshless method, which belongs to the one-level type, is promising in dealing with such one-dimensional Klein-Gordon equations.

In this paper, we propose a direct meshless method with one-level approximation, based on the radial basis functions, for the one-dimensional Klein-Gordon equations. Since the Klein-Gordon equation is time-dependent, we present two schemes for the basis functions from radial and non-radial aspects. The radial aspect is similar to the traditional radial basis functions and the non-radial aspect is a newly-proposed scheme. The first scheme is fulfilled by considering time variable as normal space variable to construct an "isotropic" space-time radial basis function. The other scheme considered a realistic relationship between space variable and time variable which is not radial. The time-dependent variable is treated regularly during the whole solution process and the Klein-Gordon equations can be solved in a direct way.

The structure of this paper is organized as follows. Followed by Section 1, we describe the one-dimensional Klein-Gordon equations with initial and boundary conditions. Section 2 introduces the space-time radial and non-radial basis functions. Followed by Section 3, we present the methodology of the direct meshless method (DMM) for the one-dimensional Klein-Gordon equations under initial condition and boundary conditions. Several numerical examples are presented to validate the accuracy and stability of the proposed algorithms in Section 4. Some conclusions are given in Section 5 with some additional remarks.

1 One-Dimensional Klein-Gordon Equation

In this paper, we consider the general mathematical formulation of one-dimensional Klein-Gordon equation

$$\frac{\partial^2 u}{\partial t^2}+\alpha\frac{\partial^2 u}{\partial x^2}+\beta u+\gamma u^2=f_1(x,t),\ a<x<b,\ t>0 \quad (1)$$

in terms with the initial conditions

$$u(x,t)=f_2(x,t), \frac{\partial u(x,t)}{\partial t}=f_3(x,t),\ t=0,\ a<x<b \quad (2)$$

and boundary conditions

$$u(x,t)=f_4(x,t),\ x=\{a,b\},\ t>0 \quad (3)$$

2 Formulation of the Space-Time Radial and Non-Radial Basis Functions

By using traditional numerical techniques, Eqs. (1)-(3) can be solved by using the two-level finite difference approximations or integral transform methods. In order to overcome the two-level strategy, direct meshless methods by using space-time radial and non-radial basis functions were worthy to be proposed.

As is known to all, the radial basis functions (RBFs) are "isotropic" for Euclidean spaces. For steady-state problems, the approximate solution can be written as a linear combination of RBFs with 2D or higher dimensions. Take the famous Multiquadric (MQ) RBF as an example

$$\varphi_{\mathrm{MQ}}(r_j)=\sqrt{1+(\varepsilon r_j)^2} \quad (4)$$

where $r_j=\left\| X-X_j \right\|$ is the Euclidean distance between two points $X=(x,y)$ and $X_j=(x_j,y_j)$, ε is the RBF shape parameter.

However, there is only one space variable x for the one-dimensional Klein-Gordon equation, the traditional RBFs are inapplicable in the direct sense. For this reason, we propose a simple meshless method by combining the space variable x and time variable t from the perspective of radial and non-radial. More specifically, the interval $[a,b]$ is evenly divided into segments firstly $a=x_0<x_1<\cdots<x_n=b$ with corresponding finess $h=(b-a)n$. The time variable is evenly chosen from the initial time $t_0=0$ to a final time $t_n=T$ as $0=t_0<t_1<\cdots<t_n=T$ with time-step $\Delta t=T/n$. The corresponding configuration of the space-time coordinate is shown in Fig. 1. Then the space-time radial basis function can be constructed as

$$\varphi_{\mathrm{MQ}}(r_j)=\sqrt{1+c^2 {r_j}^2} \quad (5)$$

$r_j=\left\| P-P_j \right\|$ is the Euclidean distance between two points two points $P=(x,t)$ and $P_j=(x_j,t_j)$. Besides, it is possible to construct the space-time non-radial basis function which has the following expression

$$\varphi_{\text{NMQ}}(r_j)=\sqrt{1+(x-x_j)^2+c^2(t-t_j)^2} \tag{6}$$

where c is a parameter which reflects a realistic relationship between space variable x and time variable t.

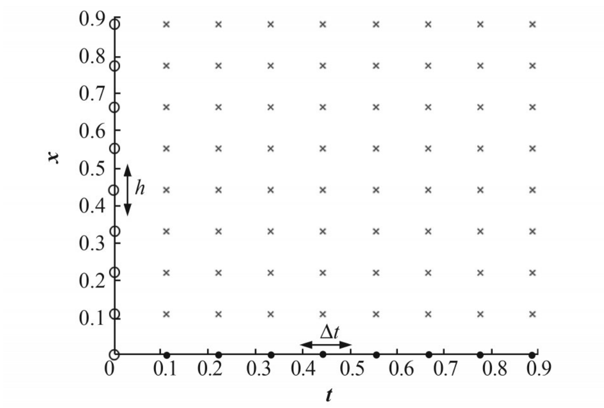

Fig.1 Configuration of the space-time coordinates

"○" stands for the value of space variable [x], "•" stands for the value of time variable [t] and "×" stands for the point [(x,t)]

We note that the space-time non-radial basis function which is product of two positive definite functions on space dimension and time dimension is investigated in Refs.[26-27]. For the MQ case, one has

$$\bar{\varphi}_{\text{NMQ}}(r_j)=\sqrt{1+c^2(x-x_j)^2}\sqrt{1+c^2(t-t_j)^2} \tag{7}$$

However, the corresponding numerical results are not well in dealing with the problems in this research.

For two-dimensional cases, the space-time radial and non-radial basis functions can be easily obtained

$$\varphi_{\text{MQ}}(r_j)=\sqrt{1+c^2r_j^2} \tag{8}$$

$$\varphi_{\text{NMQ}}(r_j)=\sqrt{1+(x-x_j)^2+(y-y_j)^2+c^2(t-t_j)^2} \tag{9}$$

Here $r_j=\left\|P-P_j\right\|$ is the Euclidean distance between two points two points $P=(x,y,t)$ and $P_j=(x_j,y_j,t_j)$.

3 Implementation of the Direct Meshless Method (DMM)

Here, we consider the initial boundary value problem Eqs. (1)-(3) to illustrate the direct meshless method (DMM). Based on the definition of space-time radial and non-radial basis functions, Eqs. (1) - (3) can be solved directly in a one level approximation. The approximate solution of the function $u(x,t)$ has the form

$$\bar{u}(\cdot)\approx\sum_{j=1}^{N}\lambda_j\varphi_j(\cdot) \tag{10}$$

with $\{\lambda_j\}_{j=1}^{N}$ the unknown coefficients.

To illustrate the direct meshless method, we choose collocation points on the whole physical domain which include N_{I} internal points $\{P_i=(x_i,t_i)\}_{i=1}^{N_{\text{I}}}$, N_{t} initial boundary points $\{P_i=(x_i,t_i)\}_{i=N_{\text{I}}+1}^{N_{\text{I}}+N_{\text{t}}}$ and N_{b} boundary points $\{P_i=(x_i,t_i)\}_{i=N_{\text{I}}+N_{\text{t}}+1}^{N}$. According to the traditional collocation approach, substituting Eq. (10) into Eqs. (1)-(3), we have the following equations

$$\sum_{j=1}^{N}\lambda_j L\varphi_j(P_i,P_j)=f_1(P_i),\ i=1,\cdots,N_{\text{I}} \tag{11}$$

$$\sum_{j=1}^{N}\lambda_j\varphi_j(P_i,P_j)=f_2(P_i),\ i=N_{\text{I}}+1,\cdots,N_{\text{I}}+N_{\text{t}} \tag{12}$$

$$\sum_{j=1}^{N}\lambda_j\frac{\partial\varphi_j(P_i,P_j)}{\partial t}=f_3(P_i),\ i=N_{\text{I}}+N_{\text{t}}+1,\cdots,N_{\text{I}}+2N_{\text{t}} \tag{13}$$

$$\sum_{j=1}^{N}\lambda_j\varphi_j(P_i,P_j)=f_4(P_i),\ i=N_{\text{I}}+2N_{\text{t}}+1,\cdots,N \tag{14}$$

where $L\varphi=\frac{\partial^2\varphi_j}{\partial t^2}+\alpha\frac{\partial^2\varphi_j}{\partial x^2}+\beta\varphi_j+\gamma\varphi_j{}^2$. We note that the initial boundary points are used twice to cope with initial conditions. Thus, the number of total collocation points $N=N_{\text{I}}+2N_{\text{t}}+N_{\text{b}}$.

Hence we should seek for the solution of the following $N\times N$ linear algebraic system

$$\boldsymbol{AX}=\boldsymbol{f} \tag{15}$$

where

$$\boldsymbol{A}=\begin{bmatrix}A_{11}&A_{12}&A_{13}&A_{14}\\A_{21}&A_{22}&A_{23}&A_{24}\\A_{31}&A_{32}&A_{33}&A_{34}\\A_{41}&A_{42}&A_{43}&A_{44}\end{bmatrix} \tag{16}$$

is $N\times N$ known matrix. $\boldsymbol{X}=\{\lambda_1,\lambda_2,\lambda_3,\lambda_4\}'$ and $\boldsymbol{f}=\{f_1,f_2,f_3,f_4\}'$ are $N\times1$ vectors.

Eq. (15) can be solved by the backslash computation in MATLAB codes. From the above procedures, we can find that the implementation of the proposed direct meshless method is very simple.

4 Numerical Simulations

To compare with the previous literatures, we consider using the maximum error(ML), absolute error and root mean square error (RMSE)[28,29] defined as below:

$$\text{RMSE}=\sqrt{\frac{1}{N_t}\sum_{k=1}^{N_t}\left|u(P_k)-\bar{u}(P_k)\right|^2} \tag{17}$$

where $u(\cdot)$ is the analytical solution at test points $\{P_k\}_{k=1}^{N_t}$ and $\bar{u}(\cdot)$ is the numerical solutions at the test points $\{P_k\}_{k=1}^{N_t}$. N_t is the number of test points on the physical domain. The optimal choice of RBF parameter is beyond the scope of our current research. For more details about this topic, readers can be referred to Refs.[30,31] and references therein. The shape parameter $c=1$ is chosen prior to numerical results.

For simplicity, we denote the space-time radial basis function Eq. (5) and space-time non-radial basis function Eq. (6) as DMM1 and DMM2, respectively.

4.1 Example 1

Here, we consider an example of the one-dimensional Klein-Gordon equation with parameters $\alpha=\beta=1$ and $\gamma=0$, i. e., $\frac{\partial^2 u}{\partial t^2}+\frac{\partial^2 u}{\partial x^2}+u=0,\ 0<x<1,\ t>0$. The corresponding exact solution is given as

$$u(x,t)=\sin x+\cosh t \tag{18}$$

which has a series form

$$u(x,t)=\sin x+1+\frac{t^2}{2!}+\frac{t^4}{4!}+\frac{t^6}{6!}+\cdots \tag{19}$$

with the following initial conditions

$$u(x,0)=\sin x+1,\quad u_t(x,0)=0 \tag{20}$$

and boundary conditions

$$u(0,t)=\cosh t,\quad u(1,t)=\sin 1+\cosh t \tag{21}$$

The corresponding source function is $f_1(x,t)=0$.

Numerical results of the DMM are listed in Table 1 with the final time $T=1$. We note that our time step $h=\Delta t=1/15$, which leads to less computations, is far larger than the one $dt=0.000\,1$ in Refs.[25, 32]. It is clear from Table 1 that the two schemes of the DMM give the same or better accuracy compared to the numerical procedures reported in Refs.[25, 32].

Table 1 Numerical comparison of the maximum errors L_∞ (ML) for example 1

t	DMM1	DMM2	FEDF[25]	MQRK4[32]	MQS[32]
0.1	4.63E−06	5.53E−06	4.25E−06	1.90E−06	2.83E−05
0.5	1.17E−05	9.63E−06	3.18E−05	8.17E−05	8.61E−05
1	9.33E−06	1.19E−05	8.90E−05	3.19E−04	3.95E−05

Table 2 shows the time convergence rate in terms of the L_∞ and L_2 error norms for the different time step sizes $\Delta t=0.1, 0.05, 0.01, 0.005$ for fixed point parameter $n=15$. From Table 2, we can find that the two schemes of the DMM perform better than the forward Euler difference formula (FEDF) in Ref.[25].

Table 2 Time convergence results of the maximum errors L_∞ and L_2 errors for example 1

Δt	DMM1		DMM2		FEDF[25]	
	L_∞	L_2	L_∞	L_2	L_∞	L_2
0.1	7.63E−05	3.98E−05	9.20E−03	6.90E-03	1.94E−02	9.76E−03
0.05	7.43E−05	2.32E−05	1.08E−06	2.69E−06	5.73E−03	3.16E−03
0.01	9.17E−06	2.99E−06	4.24E−06	2.27E−06	1.05E−03	5.72E−04
0.005	2.08E−05	7.00E−06	6.59E−06	1.34E−06	5.10E−04	2.63E−04

For fixed parameter $h=\Delta t=1/15$, the numerical results obtained by the DMM for a long range of shape parameter value c, are shown in Fig. 2 for Example 1. Less sensitivity to the selection of the shape parameter c in the case of the DMM2, in comparison to the DMM1, can be observed from Fig. 2. But the quasi-optimal parameter c for the DMM1 is near the number $c=1$.

The numerical results obtained by the DMM for the point parameter value n are shown in Fig. 3. It can be seen that solutions of the two DMM schemes consistently converge very quickly from Fig. 3. For example, the convergence rate for the square plate is about 9 for both DMM1 and DMM2 before reaching the minimum relative error value.

4.2 Example 2

In this example, we consider the one-dimensional Klein-Gordon equation with parameters $\alpha=-1$, $\beta=-2$ and $\gamma=0$, i. e., $\frac{\partial^2 u}{\partial t^2}-\frac{\partial^2 u}{\partial x^2}-2u=-2\sin x\sin t,\ 0<x<\pi/2,\ t>0$. The corresponding exact solution is given as

$$u(x,t)=\sin x\sin t \tag{22}$$

with the following initial conditions

$$u(x,0)=0,\ u_t(x,0)=\sin x \tag{23}$$

and boundary conditions

$$u(0,t)=0,\ u(\pi/2,t)=\sin t \tag{24}$$

and the source function $f_1(x,t)=-2\sin x\sin t$.

Numerical results of the DMM are listed in Table 3 with the final time $T=\pi/2$. We note that our time step $h=\Delta t=1/15$, which leads to less computations, is larger

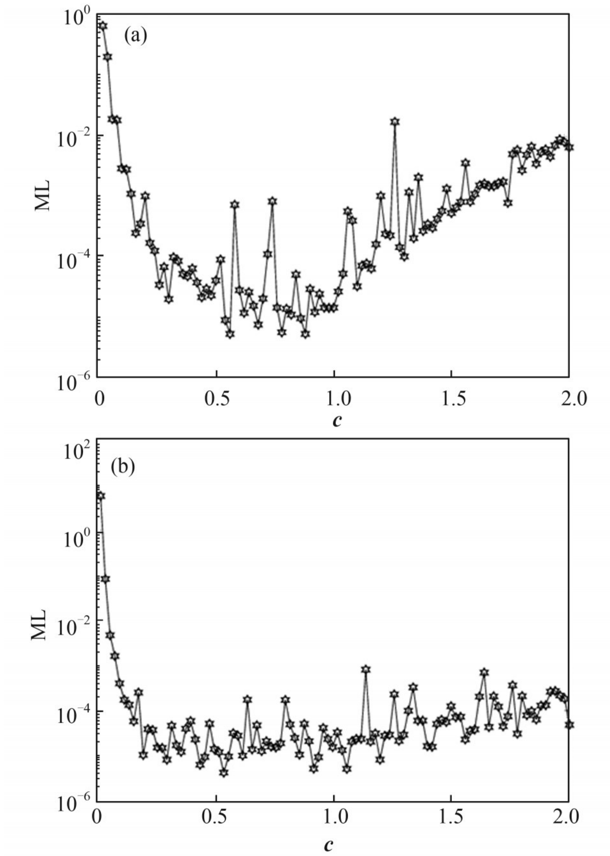

Fig.2 Shape parameter *c* versus the ML of the DMM1 (a) and DMM2 (b)

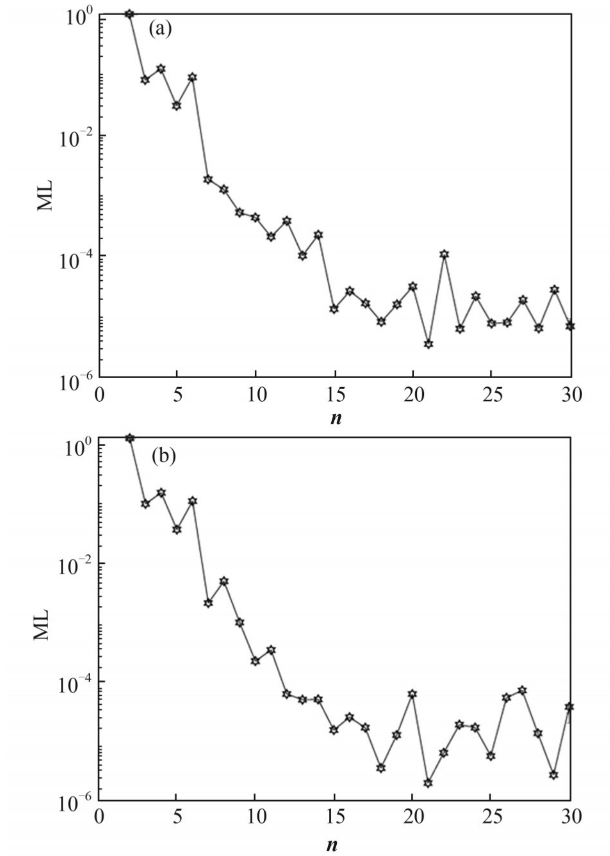

Fig.3 Point parameter *n* versus the ML of the DMM1 (a) and DMM2 (b)

than the one $dt = 0.000\,1$ in Refs. [25, 32, 33]. It is clear from Table 3 that the two schemes of the DMM give the same or better accuracy compared to the numerical procedures reported in Refs. [25, 32, 33]. Meanwhile the DMM results are more stable than the other methods for different time $t = 0.5, 0.1, 1$.

For fixed parameter $h = \Delta t = 1/15$, the numerical results obtained by the DMM for a long range of shape parameter value *c*, are shown in Fig. 4. Less sensitivity to the selection of the shape parameter *c* in the case of the DMM1, as well as DMM2, can be observed from Fig. 4. The quasi-optimal parameter *c* for the DMM1 is near the number $c = 1$ which is similar to the previous example.

The numerical results obtained by the DMM for the point parameter value *n* are shown in Fig. 5. It is shown that the DMM solutions consistently converge very quickly. Before reaching the minimum relative error value, the convergence rate for the square plate is about 9 for both DMM1 and DMM2. Table 4 shows the time convergence rate in terms of the L_∞ and L_2 error norms for the different time step sizes $\Delta t = 0.1, 0.05, 0.01, 0.005$, $n = 25$. From Table 4, we can find that the two schemes of the DMM perform better than the FEDF in Ref.[25].

Table 3 Numerical comparison of the maximum errors L_∞ for example 2

t	DMM1	DMM2	FEDF[25]	MQRK4[32]	MQS[32]	Ref.[33]
0.1	4.06E−07	3.53E−07	2.92E−07	1.50E−05	2.92E−04	5.40E−05
0.5	7.32E−07	5.21E−07	3.32E−05	8.84E−05	1.07E−02	1.20E−03
1	9.82E−07	5.18E−07	8.90E−05	5.20E−05	2.34E−02	4.30E−03

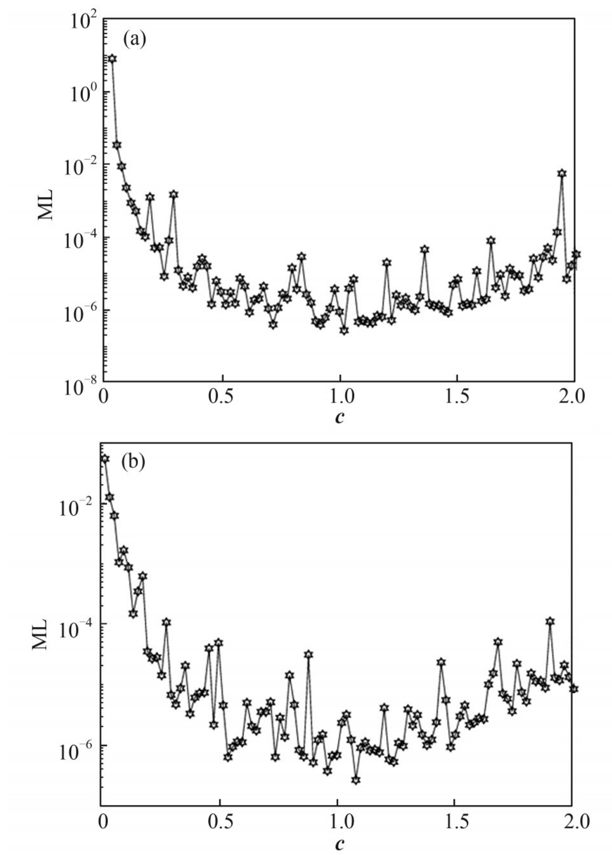

Fig.4 Shape parameter *c* versus the ML of the DMM1 (a) and DMM2 (b)

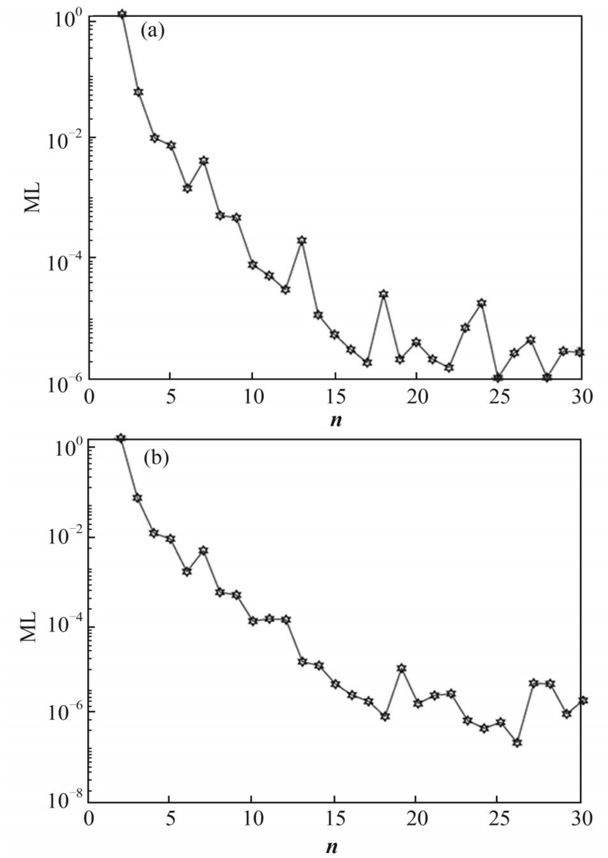

Fig.5 Point parameter *n* versus the ML of the DMM1 (a) and DMM2 (b)

Table 4 Time convergence results of the maximum errors L_∞ and L_2 errors for example 2

Δt	DMM1		DMM2		FEDF[25]	
	L_∞	L_2	L_∞	L_2	L_∞	L_2
0.1	1.10E−03	5.00E−04	5.80E−05	2.22E−05	1.65E−04	1.40E−04
0.05	1.20E−06	4.28 E−07	2.31E−06	6.05E−07	4.14E−05	3.52E−05
0.01	8.78E−07	2.40E−07	1.72E−06	7.71E−07	2.09E−06	1.68E−06
0.005	3.31E−06	1.19E−06	3.38E−06	1.02E−06	7.49E−07	6.11E−07

5 Conclusion

In this paper, a new direct meshless method is proposed for the one-dimensional Klein-Gordon equations. Two schemes are proposed for the basis functions from radial and non-radial aspects. The first scheme is fulfilled by considering time variable as normal space variable to construct an "sotropic" space-time radial basis function. The other scheme considered a realistic relationship between space variable and time variable which is not radial. Both schemes for the proposed meshless method are simple, accurate, stable, easy-to-program and efficient for the Klein-Gordon equations. More importantly, the proposed method can be used to nonlinear problems accompanied with iteration methods. The theory of our DMM procedure can be directly applied to wave propagation, transient heat transfer and thermoelastic problems with high dimensions. Also, it is promising in dealing with fractional equations [34,35].

Moreover, there is much theoretical investigation that needs to be done in this area of numerical analysis. This will be studied in the near future.

References

[1] Animasaun I L, Shah N A, Wakif A, *et al*. *Ratio of Momentum Diffusivity to Thermal Diffusivity*: *Introduction*, *Meta-analysis*, *and Scrutinization*[M]. New York: Chapman and Hall/CRC, 2022.

[2] Cao W H, Animasaun I L, Yook S J, *et al*. Simulation of the dynamics of colloidal mixture of water with various nanoparticles at different levels of partial slip: Ternary-hybrid nanofluid[J]. *Inter J Commun Heat Mass*, 2022, **135**: 106069.

[3] Xia W F, Animasaun I L, Wakif A, *et al*. Gear-generalized differential quadrature analysis of oscillatory convective Taylor-Couette flows of second-grade fluids subject to Lorentz and Darcy-Forchheimer quadratic drag forces[J]. *Inter J Commun Heat Mass*, 2021, **126**: 105395.

[4] Chowdhury M S H, Hashim I. Application of homotopy-perturbation method to Klein-Gordon and sine-Gordon equations[J]. *Chaos Soliton Fract*, 2009, **39**: 1928-1935.

[5] Wazwaz M A. New travelling wave solutions to the Boussinesq and the Klein-Gordon equations[J]. *Commun Nonlinear Sci Numer Simul*, 2008, **13**: 889-901.

[6] Zheng H, Zhang C Z, Wang Y S, *et al*. A local RBF collocation method for band structure computations of 2D solid/fluid and fluid/solid phononic crystals[J]. *Int J Numer Meth Eng*, 2017, **110** (5): 467-500.

[7] Wang L H, Qian Z H. A meshfree stabilized collocation method (SCM) based on reproducing kernel approximation [J]. *Comput Method Appl M*, 2020, **371**:113303.

[8] Gu Y, Fan C M, Xu R P. Localized method of fundamental solutions for large-scale modelling of two-dimensional elasticity problems[J]. *Appl Math Lett*, 2019, **93**: 8-14.

[9] Lin J, Chen F, Zhang L J. An accurate meshless collocation technique for solving two-dimensional hyperbolic telegraph equations in arbitrary domains[J]. *Eng Anal Bound Elem*, 2019, **108**: 372-384.

[10] Lee I J. Numerical solution for nonlinear Klein-Gordon equation by collocation method with respect to spectral method[J]. *J Korean Math Soc*, 1995, **32**: 541-551.

[11] Duncan D B. Symplectic finite difference approximations of the nonlinear Klein-Gordon equation[J]. *SIAM J Numer Anal*, 1997, **34**: 1742-1760.

[12] El-Sayed S M. The decomposition method for studying the Klein-Gordon equation[J]. *Chaos Soliton Fract*, 2003, **18**: 1025-1030.

[13] Hariharan G. Haar wavelet method for solving the Klein-Gordon and the Sine-Gordon equations[J]. *Int J Nonlinear Sci*, 2011, **11**: 180-189.

[14] Pekmen B, Tezer-Sezgin M. Differential quadrature solution of nonlinear Klein-Gordon and Sine-Gordon equations[J]. *Comput Phys Commun*, 2012, **183**: 1702-1713.

[15] Lynch MAM. Large amplitude instability in finite difference approximations to the Klein-Gordon equation[J]. *Appl Numer Math*, 1999, **31**: 173-182.

[16] Guo B Y, Li X, Vazquez L. A Legendre spectral method for solving the nonlinear Klein-Gordon equation[J]. *Math Appl Comput*, 1996, **15** (1): 19-36.

[17] Li X, Guo B Y. A Legendre spectral method for solving nonlinear Klein-Gordon equation[J]. *J Comput Math*, 1997, **15** (2): 105-126.

[18] Zheng H, Wang F, Chen C S, *et al*. Improved 3D surface reconstruction via the method of fundamental solutions[J]. *Numer Mathe Theory Me*, 2020, **13**(4): 973-985.

[19] Zheng H, Xiong J G, Yuan Y, *et al*. Mixed-mode dynamic stress intensity factors by variation technique with finite block method[J]. *Eng Anal Bound Elem*, 2019, **106**: 27-33.

[20] Zheng H, Sladek J, Sladek V, *et al*. Fracture analysis of functionally graded material by hybrid meshless displacement discontinuity method[J]. *Eng Fract Mech*, 2021, **247**: 107591.

[21] Dehghan M, Shokri A. Numerical solution of the nonlinear Klein-Gordon equation using radial basis functions[J]. *J Comput Appl Math*, 2009, **230**: 400-410.

[22] Lakestani M, Dehghan M. Collocation and finite difference-collocation methods for the solution of nonlinear Klein-Gordon equation[J]. *Comput Phys Commun*, 2010, **181**: 1392-1401.

[23] Dehghan M, Mohammadi V. Two numerical meshless techniques based on radial basis functions (RBFs) and the method of generalized moving least squares (GMLS) for simulation of coupled Klein-Gordon-Schrodinger (KGS) equations[J]. *Comput Math Appl*, 2016, **71**: 892-921.

[24] Shivanian E, Jafarabadi A. An improved meshless method for solving two- and three-dimensional coupled Klein-Gordon-Schrodinger equations on scattered data of general-shaped domains[J]. *Eng Comput – GERMANY*, 2018, **34**: 757-774.

[25] Ahmad I, Ahsan M, Hussain I, *et al*. Numerical simulation of PDEs by local meshless differential quadrature collocation method[J]. *Symmetry-BASEL*, 2019, **11**(3): 394.

[26] Myers D E, Iaco S D, Posa D, *et al*. Space-time radial basis functions[J]. *Comput Math Appl*, 2002, **43**: 539-549.

[27] Liu C, Ku C, Xiao J, *et al*. A novel spacetime collocation meshless method for solving two dimensional backward heat conduction problems[J]. *CMES Comp Model Eng*, 2019, **118**(1): 229-252.

[28] Wang F Z, Chen W, Jiang X R. Investigation of regularization techniques for boundary knot method[J]. *Commun Numer Meth Eng*, 2010, **26**: 1868-1877.

[29] Wang F Z, Chen W, Ling L. Combinations of the method of fundamental solutions for general inverse source identification problems[J]. *Appl Math Comput*, 2012, **219**: 1173-1182.

[30] Fasshauer G E, Zhang J G. On choosing optimal shape parameters for RBF approximation[J]. *Numer Algorithms*, 2007, **45**: 345-368.

[31] Chen W, Hong Y X, Lin J. The sample solution approach for determination of the optimal shape parameter in the multiquadric function of the Kansa method[J]. *Comput Math Appl*, 2018, **75**: 2942-2954.

[32] El-Sayed S M. The decomposition method for studying the Klein-Gordon equation[J]. *Chaos Soliton Fract*, 2003, **18**: 1025-1030.

[33] Hussain A, Haq S, Uddin M. Numerical solution of Klein-Gordon and sine-Gordon equations by meshless method of lines[J]. *Eng Anal Bound Elem*, 2013, **37**: 1351-1366.

[34] Wang F Z, Hou E R, Salama S A, *et al*. Numerical Investigation of the nonlinear fractional Ostrovsky equation[J]. *Fractals*, 2022, **30**(5): 22401429.

[35] Wang F Z, Khan M N, Ahmad I, *et al*. Numerical solution of traveling waves in chemical kinetics: Time fractional fishers equations[J]. *Fractals*, 2022, **30**(2): 2240051.

□